

Scientific Spokesman:

J. Pine
 Charles C. Lauritsen Laboratory
 of High Energy Physics
 California Institute of Tech.
 Pasadena, California 91109

A PROPOSAL TO STUDY HIGH P_T PHYSICS
 WITH A MULTIPARTICLE SPECTROMETER

G. Fox, R. Gomez, J. Pine
 California Institute of Technology, Pasadena, California

E. Lorenz, P. Schlein, W. Slater, R. Webb
 University of California, Los Angeles, California

R. Abrams, S. Bernstein, H. Goldberg, S. Margulies,
 D. McLeod, J. Solomon
 University of Illinois, Chicago Circle, Chicago, Illinois

D. Dzierba, J. Martin
 University of Indiana, Bloomington, Indiana

V. Ashford, E. Malamud, A. Wehmann, *Kubala, Mori, Haggerty*
 National Accelerator Laboratory, Batavia, Illinois

October 1973

Pine

A PROPOSAL TO STUDY HIGH p_T PHYSICS
WITH A MULTIPARTICLE SPECTROMETER

G. Fox, R. Gomez, J. Pine
California Institute of Technology, Pasadena, California

E. Lorenz, P. Schlein, W. Slater, R. Webb
University of California, Los Angeles, California

R. Abrams, S. Bernstein, H. Goldberg, S. Margulies, D. McLeod,
J. Solomon
University of Illinois, Chicago Circle, Chicago, Illinois

A. Dzierba, J. Martin
University of Indiana, Bloomington, Indiana

V. Ashford, E. Malamud, A. Wehmann
National Accelerator Laboratory, Batavia, Illinois

Spokesman: J. Pine

Abstract

The multiparticle spectrometer system, now being constructed for Experiment 110, is to be used at 200 Gev to gain a global view of interactions in which one or more particles carry off high values of p_T . The spectrometer will give 4π acceptance for detection of charged particles, and large solid angle for momentum measurement and particle identification. Several triggers are discussed, but the main emphasis is on calorimeters (designed for gamma ray and hadron showers) which detect high p_T particles, or groups of particles, over a large part of the c.m. angular range from 0 to 120 degrees. The apparatus is expected to give very detailed information in the p_T range from about 2-6 Gev/c, from rates estimated on the basis of known single particle inclusive cross sections, measured near 90 degrees in the center of mass. In addition, the experiment will study events with high p_T forward-going systems, where little experimental information now exists, but where very interesting questions can be studied.

I. INTRODUCTION

Originally at the ISR¹⁾, and more recently at NAL²⁾, surprisingly large single-particle inclusive cross sections have been observed at high values of transverse momentum. The exponential p_T distribution up to 1 GeV/c apparently becomes a power law [perhaps like $(1/p_T)^8$] at higher values of p_T . The change apparently sets in at about 2 GeV/c, and by 3 GeV/c the inclusive pion cross section is more than an order of magnitude above the extrapolated exponential. This has been observed by Cronin et al., at 200 GeV at NAL, and indications are, from the data of Carey et al. at NAL, that this high p_T phenomenon is important above about 100 GeV.

The interest in these results has been intensified by the interpretation, in terms of the parton model, that the high transverse momentum particles are the result of hard parton-parton collisions. Various theoretical models have been constructed, to try to describe such interactions³⁾, and to fit the observed data. While the parton picture is qualitatively appealing, the theories are in no sense fully detailed. Many fundamental questions remain even if the qualitative picture is right. Furthermore, there is the possibility that a different, non-parton, qualitative picture is more correct.

The inclusive data do indicate beyond a doubt that something new is being observed. In terms of the parton picture, the new phenomena may be very fundamental. However, regardless of theoretical speculations, the purely experimental question of what the entire interaction looks like when one of these high p_T particles is emitted is very interesting. This is a proposal to use the Experiment 110 multi-particle spectrometer to look at such interactions with essentially 4π solid angle.

The spectrometer, as it is now being constructed, is a complex system, designed to study the peripheral physics of multi-particle systems in full detail. Fig. 1 shows a schematic view of this apparatus, and a full discussion of its attributes appears later in Section III. In terms of approximate ranges of angles in the c.m., at an incident energy of 200 GeV, the major attributes of the spectrometer relevant to this proposal are as follows:

Angular Range (extending both ways from 0 degrees)	Performance
0-180	Measure charged particle directions; some knowledge of gamma ray multiplicity.
0-120	Measure charged particle momenta. Identify particle masses with one threshold Cerenkov counter.
0-100	Measure charged particle momenta. Identify masses with two successive threshold Cerenkov counters.

Momentum measurements, and particle identification, are available for $3/4$ of the total c.m. range of $\cos\theta$. However, the table above refers to the horizontal aperture of the system, while the vertical aperture is somewhat smaller. For momentum measurements and particle identification with the first Cerenkov counter, the vertical c.m. angular range is 0-90 degrees. For the second Cerenkov counter, the vertical

range is about 0-60 degrees.

In order to use the powerful system summarized above most effectively to study high p_T physics, we have come to the conclusion that calorimeter triggering is best. The main reason is that this trigger can respond to the known single-particle yields of both pions and nucleons, including neutrons and π^0 's as well as charged particles. In addition, the calorimeters described here will allow triggering on high p_T particle clusters, such as might come from resonance decay. These trigger calorimeters will also provide good acceptance for a very large range of the variables x and p_T . While the high p_T data that stimulates this proposal is mainly limited to small x (i.e., angles in the neighborhood of 90° in the c.m.), the study of events with high p_T for large x is also very interesting.

With the M6 beam, it will be possible to study high p_T physics for a variety of incident beam particles, and with the Cerenkov counters of the spectrometer, as well as with the calorimeters, to identify a variety of secondary particle types. The proposed setup therefore has good potential for studying this physics in great detail. In the succeeding sections, we will consider more fully various aspects of the experiment. An outline of these discussions is as follows:

- Section II. Design motivation. Questions of beam energy and particle type, ability to detect jets if they exist, interest in high p_T physics away from 90° c.m. as well as near 90° .
- Section III. Apparatus. The spectrometer system; the proposed triggering calorimeters.
- Section IV. Acceptances, estimated rates, and logistics for performing the experiment.

II. Design Motivation

In this section we will describe the general considerations which motivate our experimental design. First, high energy is desirable, because the acceptance of the apparatus is better and because observations indicate that the high p_T cross section increases with energy at fixed p_T . We believe that the M6 beam will deliver excellent fluxes of protons and pions at 200 GeV/c, and in the rest of this section we concentrate on this energy.

It is worth discussing first whether 200 GeV/c is really a high enough energy. The inclusive data of Carey et al (3,4) for photons presumably from π^0 's shows that between 50 and 100 GeV/c incident energy a break in $\frac{d\sigma}{dp_T d\Omega}$ develops at $p_T \approx 1$ GeV/c. Parametrizing this as

$$\frac{d\sigma}{dp_T d\Omega} = A \exp[-B p_T + C p_T^2]$$

the NAL group find a B value that is roughly energy independent, while the coefficient C jumps from around 0 at 50 GeV/c to .3-.5 in the range 100 to 400 GeV/c. Identifying the non-zero value of C with the new high p_T phenomenon, we find that at 100 GeV/c and $p_T = 2$ GeV/c it is already three times higher than the simple exponential seen at 50 GeV/c. The dominance of the new term increases rapidly as either energy or p_T are increased. We deduce that studies at 200 GeV/c and $p_T \gtrsim 2$ GeV/c will thus be very sensitive to the new high p_T phenomenon.

A similar conclusion may be reached from the phenomenological form, suggested by the interchange model: (5)

$$E \frac{d^3\sigma}{dp^3} \sim \frac{1}{(p_T)^2} \exp\left[-\gamma p_T / \sqrt{s}\right],$$

with $y \approx 28$, which describes the current data at 200 GeV/c and above.^{2,4} The rise with s at fixed p_T comes from the exponential $\exp[-y p_T / \sqrt{s}]$, which at $p_T = 2$ GeV/c takes the values .02, .06, and .1 at $p_{\text{lab}} = 100, 200, \text{ and } 300$ GeV/c respectively. Given the appearance, and indeed dominance, of the new high p_T phenomenon as low as 100 GeV/c, we conclude that both 200 and 300 GeV/c beams are excellent tools, with the latter offering no apparent qualitative advantages but somewhat higher rates.

In the meson lab, the possibility of intense beams at 300 GeV/c (except for protons) depends on the ability to target at 400 GeV/c, a problematical question. Moreover, it must be admitted that the M6 beam will not be easy to raise above 200 GeV/c, while the M1 beam will be much easier to modify to around 300 GeV/c. However, considering the power which can be brought to bear on the high p_T physics by the multi-particle spectrometer, and the expectations of quite satisfactory data rates (see Section IV), we do not believe that the shortcomings of the M6 beam in either energy or intensity are dominant factors.

In common with other meson lab experiments, this proposal embodies the advantages of observing the effect of different incident beam particles. In the quark-parton models, (6,7) for example, the high p_T amplitude depends on the constituent quarks of beam and target particles. Not only is the final state composition expected to depend on beam and target species, but in many theories the high p_T cross section is expected to be larger for incident mesons than for incident baryons. It is also interesting to utilize both hydrogen and deuterium targets, for similar reasons.

From general principles, high p_T single particle inclusive scattering can be labelled with the x and p_T , or equivalently the θ_{cm} or θ_{lab} and p_T , of the produced particle. These are only restricted by the approximate inequality $p_T^2 \leq \left(\frac{5(1-x^2)}{4} \right)$ and for this

range Fig. 5 indicates (at 200 Gev) the relation between the variables x , θ_{cm} , and θ_{lab} .

We wish to study high p_T phenomena over as large a part of the kinematic range as possible. As discussed in Section I, the experiment 110 spectrometer allows magnetic analysis for particles emitted with $\theta_{cm} \leq 120^\circ$. We expect this coverage to permit study of most of the interesting physics.

It is convenient to divide the region $\theta_{cm} \leq 120^\circ$ into two parts: First, there is $60^\circ \leq \theta_{cm} \leq 120^\circ$ or the $x \approx 0$ region (hereafter called the 90° region). Secondly, there is the small θ_{cm} or high x ($\geq .4$) region (hereafter called forward). This distinction is useful because we propose separate triggers sensitive to one or the other of these regions and also because at present there is experimental data for high p_T in the 90° region but not the other.

We will trigger on high p_T particles traversing the magnet (either singly or in a cluster), and then use the spectrometer to obtain a global view of the interaction. Independent of any model, from momentum conservation, the observation of high p_T on one side of the beam direction requires balancing in the opposite hemisphere. The only possibilities appear to be other high p_T particles or an increased multiplicity of low p_T ones. The spectrometer can be used to study either case in detail and to reveal which, if either, is the dominant behavior.

If the high p_T process is reflected by target and projectile fragmentations which are in some way unusual, the spectrometer can also reveal this. The projectile fragmentation, in the the forward direction, is extremely well analyzed. The target fragmentation detectors will yield direction and multiplicity data. A further strong point of the spectrometer is the ability to study high p_T resonance formation. Resonance decays, in addition to single particles, may in fact contribute to the observed single particle inclusive rates.

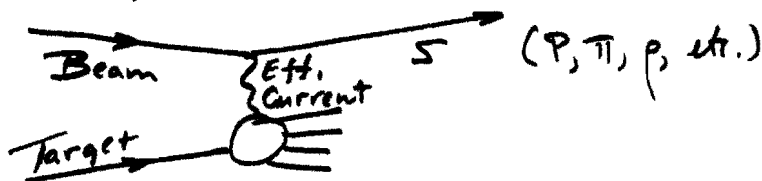
Let us now consider in greater detail some theoretical possibilities for events corresponding to high p_T in the 90° region. While experimental information is still very incomplete, a variety of rather qualitative theoretical models have been proposed to help interpret the data in this region. One which is particularly appealing, but not without difficulties, is the hard parton interaction model. ^(6,7) Here, two partons emerge in roughly opposite directions in the overall c.m. system, each with high p_T , and then fragment into what have been called hadron "jets". More precisely, the decay hadrons from a single high p_T parton are asserted to have momentum $z \vec{p} + \vec{q}$, where \vec{p} is the parton c.m. momentum, z has a smooth distribution peaking like dz/z at $z=0$, and \vec{q} ~~is a vector transverse to \vec{p}~~ with magnitude $\lesssim 300$ MeV/c. Such decay hadrons transform into a cone (jet) of particles subtending about ± 20 mrad in the lab. This angle is small compared to the spectrometer acceptance and so our apparatus will be splendid for examining such events.

We have used the detailed model of Ellis and Kislinger ⁽⁷⁾ to make these statements more quantitative. For one high p_T particle observed at 100 mrad (the trigger particle), we find about 80% probability that the "recoil" jet is detected. Over the full aperture for trigger particles, extending from 50 to 150 mrad, the probability of seeing the correlated jet remains greater than 50% everywhere. Note that at the modest p_T 's ($p_T \lesssim 5$ GeV/c) that we can study, a jet is two to (optimistically) four large p_T particles travelling at similar lab angles.

Actually there are many other theoretical models, even when we stick to a quark-parton picture. For instance, in the Ellis-Kislinger model, the hadron decay products of the parton peak along the parton direction in the original beam-target c.m. system. Another possibility is for the decay hadrons to come from a final-state interaction between the parton and the "core" remaining after removal of a parton from either the target or beam particle.

Such hadrons would peak in the parton-core c.m. and would be experimentally very distinct (being of higher multiplicity and at smaller lab angles) from the jets of the Ellis-Kislinger model.

Now, let us turn to the high x , or forward, region. Many models suggest an analogy between this and electroproduction $e + N \rightarrow e + \text{anything}$, where the photon exchange is replaced by an "effective current" ⁽⁵⁾, as sketched below:



This analogy is perhaps particularly appealing when the particle s , scattered at high p_{\perp} , is of the same type as the incident beam. As there is essentially no data in this region to even determine phenomenological parameters, the theories are very speculative, and one must design the experiment to cover the widest range of possibilities.

The process $p + p \rightarrow p + \text{anything}$ has been measured up to $p_{\perp} = 1.5 \text{ GeV}/c$ and equivalent $p_{\text{lab}} = 500 \text{ GeV}/c$, at the ISR. ⁽⁸⁾ For $x \gtrsim 0.9$, the cross section ($E(d^3\sigma/dp^3) \approx 3\mu\text{b}/\text{GeV}^2$) is much smaller than at $x = 0$ (even though at small p_{\perp} , in the diffractive region, the opposite is true). For this reason, we wish to be able to make the forward trigger sensitive to smaller p_{\perp} than the 90° trigger (where we nominally expect to set a lower limit of $2 \text{ GeV}/c$). In fact, the apparatus will be sufficiently flexible so that if the above rates are misleading the trigger can be conveniently adjusted to a larger or smaller threshold p_{\perp} .

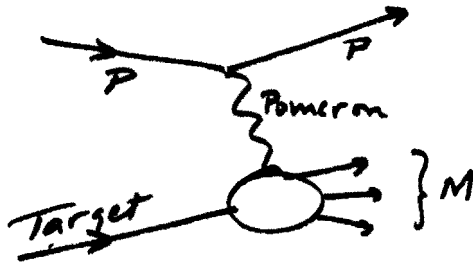
Theoretically, the reduction in cross section for very large x ($\gtrsim 0.9$) is not unexpected. For instance, in the interchange model, the invariant cross section is proportional to $(1-x)^{2(n_B + n_S) - 1}$ for fixed p_{\perp} and x near 1. Here n (subscripted B for beam and S for scattered particle) takes the value 1 for mesons and 2 for baryons.

This intriguing particle dependence also illustrates the importance of studying the phenomena with all possible beams and scattered particles.

Returning to the electroproduction analogy, there is great interest in the final hadron distribution for inelastic electron scattering ⁽⁹⁾. How do the partons disintegrate into hadrons without giving observable particles with quark quantum numbers? The models which say there is a qualitative relation between deep inelastic electron scattering and high p_{T} hadron processes suggest this is solved in the same way in both reactions. Whether or not they are right, study of the hadron process is not only interesting in its own right but can be usefully compared with electronproduction.

A final use of the forward high p_{T} trigger is to include the study of such homely processes as $pp \rightarrow pN^*$, or even high p_{T} elastic scattering. At 200 Gev/c, ISR data suggests about 0.1 microbarn of cross section for elastic pp scattering at $p_{\text{T}} \geq 1.5$ Gev/c. ⁽¹⁰⁾ At 24 Gev/c, the total N^* production with masses ≤ 2.5 Gev is about ten times this. ⁽¹¹⁾ Again, a minimum p_{T} of about 1.5 Gev/c leads to possibly interesting rates.

Pictorially, this type of physics can be viewed as a study of pomeron-proton scattering as a function of M^2 and p_{T} :



This has been studied at low p_{T} in the NAL bubble chamber exposures and has created much interest. ⁽¹²⁾ Some hints as to interesting p_{T}

dependence come from a recent Brookhaven experiment at 28 GeV/c⁽¹³⁾, which showed that the multiplicity of the N^* decay in $pp \rightarrow pN^*$ increases with p_T in the region of N^* mass ≤ 5 GeV and $0 \leq p_T \leq 2$ GeV/c. Hopefully, by observing such processes, we can study the nature of the final states as we switch from a Pomeron exchange picture to the "effective current" exchange of the electroproduction analogy.

We want to emphasize that the experiment proposed here has not been designed to test any particular, and probably wrong, theory, but to be as broadly sensitive as possible, and hence to permit testing of the widest variety of current and future theoretical ideas. Experimental data, and current theories when data are scarce, have been used to help estimate trigger rates and possible characteristics of interesting events.

III. Apparatus

A. The Multiparticle Spectrometer

Figure 1 shows a schematic view of the spectrometer now being built for Expt. 110, with three calorimeters added. Before discussing the use of these for triggering, and other possible triggers, it is appropriate to first outline the planned performance of the remainder of the apparatus.

Beginning with the beam, proportional chamber hodoscopes will determine the directions of incoming beam particles with a standard error of about 10^{-5} radians, and their momentum to 0.1% or better. Cerenkov counters will tag particle types. The target is 50 cm. long, and it is almost fully enclosed in cylindrical proportional chambers and a cylindrical array of 24 lead-scintillator gamma counters. Other gamma counters cover the upstream and downstream regions around the target, except for a forward aperture matched to the magnet acceptance. The target detectors measure the directions of charged particles over essentially 4π solid angle. In addition, the segmented gamma counters give some information about directions and multiplicities of neutral pions.

Particles which enter the magnet are measured by both proportional and spark chambers, the intention in Expt. 110 being to use proportional chambers to determine particle multiplicities and approximate trajectories, but to rely on magnetostrictive spark chambers for most of the accurate trajectory measurements. Each spark chamber module shown in Figure 1 will have four or more gaps with both planes of each gap read out, to help achieve good multiparticle efficiency and track-finding ability.

In this proposal we will assume a maximum usable beam intensity of 2×10^6 for a one-second spill, leading to about 10^5 interactions per second. We expect

that particle trajectories will be determined under these conditions by using the spark chambers following the magnet but only proportional chambers before the magnet (owing to the relatively large number of old sparks expected in spark chambers there). The geometry is such that the momenta of particles traversing C1 will be determined with an accuracy of approximately $\pm 2\%$ at 50 GeV/c, the percentage error scaling proportional to momentum. For the physics of interest here, this accuracy, and the precision of angle determinations, is more than adequate.

The Cerenkov counters are useful for particle identification, within limits set by the available range of threshold velocities. Each is to be segmented into sixteen regions by using multiple mirrors, each focussing the light incident on it to a separate phototube. Each phototube will be pulse-height analyzed for every event. In this fashion, particle identification is expected to be practical in a significant fraction of high multiplicity events.

The maximum useful pion threshold for C1 will be about 10 GeV/c, while for C2 it will be about 20 GeV/c. At these settings, for particles traversing both Cerenkov counters, a complete π , K, P separation is expected from about 36 to 70 GeV/c, while mesons will be distinguished from protons from 36 to 140 GeV/c. For particles traversing C1 only, at a threshold of 10 GeV/c for pions, meson-proton separation is made for momenta from about 36 to 70 GeV/c. From 10 to 36 GeV/c, pions are distinguished from the sum of kaons and protons. However, by changing the gas in this counter these two regions may be shifted to lower momentum ranges.

B. Trigger Calorimeters

In Figure 1, three calorimeters are shown schematically. Each has a frontal area of approximately 1.3 square meters. Identical ones, on either side of the beam line, are intended to cover a region centered at 90° in the c.m. at

200 GeV/c, and a line with an arrow indicates the trajectory of such a 90° particle, with a transverse momentum of 2 GeV/c. These "90°" calorimeters are intended to function as triggers for one or more particles with total transverse momentum greater than about 2 GeV/c and c.m. angles from about 60° to 120° . This is the kinematic region where data on high p_T single-particle inclusive cross sections are relatively plentiful and data rates can be predicted.

Leaving a discussion of the "forward" calorimeter, which is after C2, for later, we will describe the 90° calorimeter in more detail. In order to develop reasonable resolution in p_T the frontal area of the calorimeter must be segmented. There are two reasons for requiring accuracy in p_T determination: For neutrals, the calorimeter provides the only p_T measurement. Also, either for charged particles or for neutrals, effective triggering is facilitated by the ability to establish a relatively sharp minimum p_T for the entire sensitive area of the calorimeter. In our proposed experiment this is important, since we want, if possible, to reduce the rate of uninteresting triggers to a level compatible with a spark chamber detection system. If this is not possible, then some proportional chambers will need to be added to the planned spectrometer.

A simple trial calorimeter scheme is shown in Figure 2a, utilizing fixed size modules with frontal area 21 x 80 c.m. Figure 2b indicates how a calorimeter module might be constructed. For simplicity, plastic scintillator sheets are envisioned between fixed thickness iron plates. A reasonable design would be 36 plates, each 1.5" thick, with 1/4" scintillators. The scintillators following the first 12 iron plates are to be viewed by one phototube, while the other 24 are viewed by another. Since the first 12 plates amount to about 23 radiation lengths, photon-initiated showers will be almost entirely contained in this region. The hadron-initiated showers will nearly always produce an appreciable

signal in the second phototube, though much of the energy will quite often be detected by the first phototube. The "hadron energy" signal from the module must be a properly weighted sum of the signals from both phototubes, while a "photon-energy" signal is derived from the first phototube. The relative sizes of the signals in the two phototubes are expected to make it possible to distinguish between neutrons and π^0 's, as long as they occur in roughly comparable numbers.

In order to develop a sum signal for the entire calorimeter, appropriate for triggering on some minimum value of the total p_T seen by the calorimeter, the energy signals from all the modules must be combined in an overall weighted sum. The weight factors are proportional to the mean particle angle for each segment, which differs for charged and neutral particles because of the bending of the charged particles by the magnet. Note however, that the weighting is only weakly dependent on p_T , so that a threshold p_T can simply be varied by changing the required minimum value of the weighted sum.

The performance of the calorimeter chosen as an example has been evaluated from the reports of Barish et al.¹⁵⁾ and of Engler et al.¹⁶⁾ As a rough guess, we estimate its energy resolution to be about 1.5 times worse than the one studied by Engler et al., which has 2 cm. iron plates. The combined effect of this energy resolution and the geometrical coarseness of the calorimeter segments leads to an uncertainty in p_T of from $\pm 15\%$ to $\pm 20\%$ over the full area of the device. In the trigger rate and acceptance calculations of the next section, this resolution has been used. It should be emphasized that the use of this calorimeter in the manner envisioned, leads to triggering on total incident p_T , which encompasses both single particle and particle-cluster events. Also, for charged particles the p_T accuracy of the calorimeter only affects its triggering properties, since measurements of p and θ with the spectrometer will ultimately

define p_T with high accuracy.

Turning now to the calorimeter behind C2, it is intended to cover the forward c.m. region, but not to intercept the beam or the low p_T particles carrying most of the energy from ordinary interactions. Figure 3 shows a front view of this calorimeter which has been taken as a first trial. The major problem which can be foreseen is avoiding an excessive trigger rate from low p_T particles swept transversely by the magnet. This design should probably be modified to preserve a horizontal slot through the entire area. The configuration shown was an attempt to solely use modules identical to those for the 90° calorimeters discussed above. It is likely that a more fine-grained array should be used in this case, to limit the p_T range per module to a more reasonable spread.

As in the case of the 90° calorimeter, a weighted sum of the signals from the forward calorimeter can be used to establish a threshold p_T . In addition, both here and in the case of the other calorimeters, there is flexibility in forming other sorts of sums for triggering, including single particle triggers, or those which select a particular angular range or a particular kind of signal pattern from one calorimeter. Correlations between calorimeters might also be interesting. The spectrometer trigger electronics is intended to facilitate running with several simultaneous triggers, each controlled as to its share of "live time," Thus, trials of various triggering ideas will be facilitated.

There are two other possible triggering modes which may be useful, but which we do not now consider competitive with the use of the calorimeters described so far. One is a "missing energy" scheme, utilizing a calorimeter centered on the beam line just behind the magnet. For a subtended half-angle

of about 75 milliradians, and an energy loss of perhaps 75 GeV, this appears, from our Monte Carlo studies, to be promising. However, there are two major disadvantages: lack of good analysis of the projectile fragmentation products, and high backgrounds generated by the beam striking this calorimeter. However, because the missing energy technique is uniquely unbiased, it may be quite worthwhile to try it, perhaps using calorimeter modules built primarily for the other triggers.

A second trigger utilizes C2 to provide a minimum energy threshold of 20 GeV/c for a single pion, and selects pions moving at relatively large angles by requiring signals from the phototubes for the outer mirrors of C2. In this way, it appears practical to trigger on charged pions with a minimum p_T of about 2 GeV/c. Solid angle acceptance is competitive with the 90° calorimeters. However, the trigger is limited to charged pions, and the minimum p_T cannot easily be varied. In addition, electrons with momentum $\gtrsim 70$ MeV moving at about 100 milliradians to the beam direction will also produce trigger signals in traversing C2. These may constitute a serious background, and their numbers are difficult to predict accurately. The important virtue of this trigger is that it utilizes only the standard instrumentation of the spectrometer. It is therefore easy to try, and if it works it can conveniently provide a sample of high p_T data at an early stage of the spectrometer checkout.

IV. Acceptance, Rates, Logistics

In order to evaluate the performance of the proposed calorimeter triggers, two types of calculations have been performed, which we call "response" and "acceptance" determinations. The former is an attempt to evaluate the response of the calorimeters to typical, uninteresting (from a high p_T point of view) interactions. To do this, a statistical model has been used to simulate the total interaction cross section at 200 GeV. Careful comparison¹⁴⁾ of this statistical model with both ISR and NAL data indicates that it gives at the 10% level excellent fits to multiplicity, single particle inclusive, and two particle correlation data. We feel that it provides the best representation possible at this time, of the "normal" interactions which we are trying to avoid triggering on.

The particles resulting from each interaction have been tracked through the spectrometer. The response of each calorimeter, in terms of a measured total p_T , to the particles from each interaction has been determined, and effects of the energy and geometrical resolutions have been included. Typically, the p_T range for a module had an estimated standard error of $\pm 20\%$. For 2,000 simulated interactions, the largest apparent p_T observed in any calorimeter was one event at 2.75 GeV/c. Only one other event gave an apparent p_T greater than 2.0 GeV/c. At the level of less than .1% of the total interactions, the model certainly cannot be considered a reliable guide. However, an encouraging result, such as the one found, is at least a necessary condition that the triggering scheme be practical.

In the event that uninteresting low p_T triggers are too numerous, one solution is to utilize sums over small parts of the individual calorimeters for the trigger (at lower p_T only, since edge effects will reduce the acceptance).

Our main assurance, in addition to the Monte Carlo calculation, that a reasonable lack of sensitivity to uninteresting events can be achieved is the great adaptability of the proposed system, either by means of geometry modifications or electronic selection.

By "acceptance" we mean the efficiency of the system for detecting single high p_T particles. For the 90° calorimeter, this acceptance, plus the known single-particle inclusive cross sections, leads to an estimated real data rate. In determining the acceptance, energy and angle uncertainties of the calorimeter have been included, with an estimated reasonable bias on the p_T sum of each calorimeter. The bias was selected to yield good data above about 2 GeV/c, and the resulting acceptance is shown in Figure 4.

In Figure 4 the acceptance is given as the solid angle in steradians over the range of c.m. angles from 60 to 120 degrees. For a perfect instrument, the acceptance would be 2π , while here we see it reaches about 0.4 times this value at the high values of p_T . Averaging the acceptance over θ in this way is convenient for estimating rates, since we will assume, from the ISR data, that the invariant cross section is approximately constant over this angular range.

In order to estimate rates we assume 2×10^6 particles per pulse, 900 pulses per hour, and a 50 cm. hydrogen target. The resulting rates per ten hours, utilizing the single particle pion cross sections measured at NAL and the ISR and the acceptance of Figure 4 are given in the table below.

p_T range (GeV/c)	Rate/10 hours
2-3	5×10^3
3-4	3.5×10^3
4-5	1.4×10^2
5-6	4

The rates given in the table are for a single pion charge state, so that the yield of interesting data, from all high p_T particles, is expected to be three to five times as great.

For the forward calorimeter, there is no appropriate single particle inclusive data available at present. However, the acceptance here, expressed as the fraction of azimuth covered for given θ (or given p_T and x), typically exceeds 50% for $x \gtrsim 0.6$ and $p_T \gtrsim 3$. In Figure 5, shaded areas on a kinematics plot indicate the region where the proposed calorimeters have good acceptance. "Good" is defined as near the maximum attainable for high p_T , and appreciable (greater than about 10%) for low p_T where cross sections should be larger. Near the kinematic boundary along the semicircle, the acceptance is high and determined purely by geometry, while at low values of p_T the acceptance is established electronically and can be easily varied.

In referring to the shaded areas of Figure 5 note that they solely denote the regions favored for triggers. Once a trigger has been generated, the apparatus has 4π acceptance for charged particle directions, and provides momentum measurements over the entire kinematic region forward of about 120° in the c.m. system.

If our estimates are sound, the proposed experiment should provide very valuable detailed data on many aspects of high p_T physics. In view of the expected importance of such data, we feel impelled to pursue this experiment, if it is approved, before completing Experiment 110. However, we do not think it is desirable to delay the completion of the spectrometer system because of the effort needed to prepare this experiment. A program which we feel is practical and achieves the goals noted above is as follows:

1. If this proposal is approved, we will immediately assess the resources of the participating groups to determine whether the calorimeters should be designed and built by some of us. If the available resources are not sufficient to do this without slowing down the spectrometer construction, we will seek to add an outside group to this experiment, expressly for implementing the calorimetry.
2. Assuming one or the other of the alternatives in (1) is implemented, we would plan to proceed as follows:
 - a) Spectrometer checkout runs, including both the Expt. 110 system and the added calorimetry.
 - b) First-stage high p_T experiment, provided the checkout has indicated that the experiment is feasible at this time.
 - c) First-stage multiparticle peripheral physics experiment, in parallel with data reduction of the first-stage high p_T runs.
 - d) Priorities for further running to be dictated by the results of the two first-stage runs.

Considering the data rates, we would expect to run for 100-150 hours at 200 GeV for the first-stage high p_T experiment. To pursue these high p_T studies in more detail, assuming that the first run is successful, should require another 300-500 hours. However, in view of the possibility that Expt. 110 will also produce new and unexpected results, and that the first-stage running with the spectrometer will not occur sooner than about a year from now, we do not believe it is sensible to establish relative priorities between the two experimental programs until after both initial runs.

References

1. Alper, et al., Phys. Letters 44B (1973) 521.
2. Cronin, preliminary results.
3. D.C. Carey et al., preprint (1973).
4. J.K. Walker, invited talk at 1973 Stonybrook conference and preprint (1973).
5. R. Blankenbecler, S.J. Brodsky and J.F. Gunion, Phys. Letters 42B (1972) 461.
6. J.D. Bjorken, SLAC-PUB-1280, July 1973.
7. S.D. Ellis and M.B. Kislinger, NAL-PUB-73/40, June 1973.
8. M.G. Albrow et al., preprint July 1973.
9. J.D. Bjorken, Phys. Rev. D7, (1973) 282;
R.N. Cahn and E.W. Colglazier, preprint (1973).
10. ACGHT collaboration, data from the ISR presented at 1972 Batavia-Chicago conference.
11. J.V. Allaby et al., Nucl. Phys. B52, (1973) 316.
12. G.C. Fox, invited talk at 1973 Stonybrook conference and preprint (1973).
13. A. Ramanauskas et al., BNL 18175 preprint (1973).
14. E.L. Berger and G.C. Fox, CERN-TH-1700 preprint (1973).
15. B. Barish, et al., Caltech Report CALT-68-410, Sept. 1973.
16. J. Engler, et al., Nucl. Instr. and Meth., 106, (1973) 189.

SCHEMATIC PLAN VIEW - EXP. IIO MULTIPARTICLE SPECTROMETER

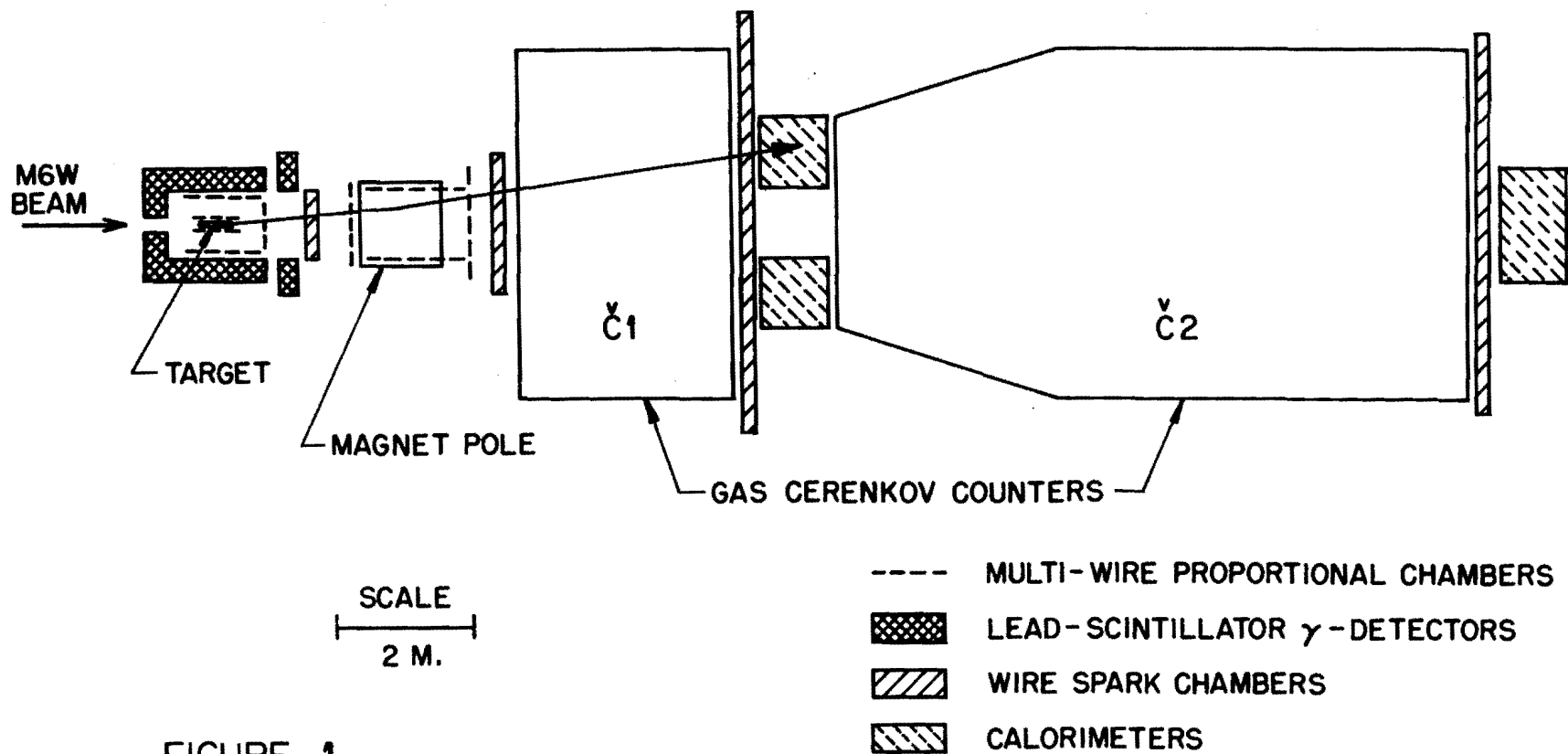
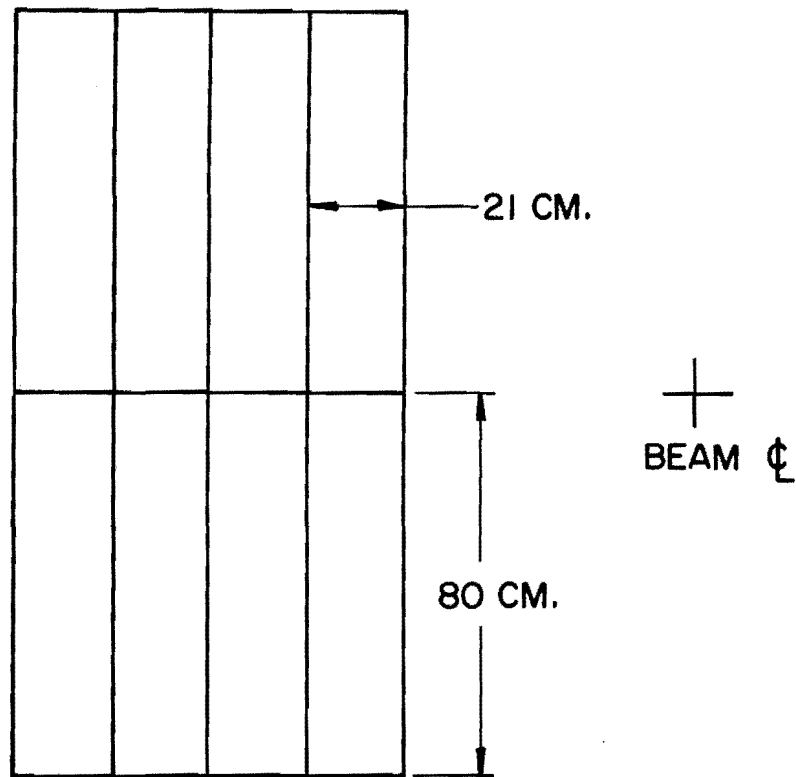
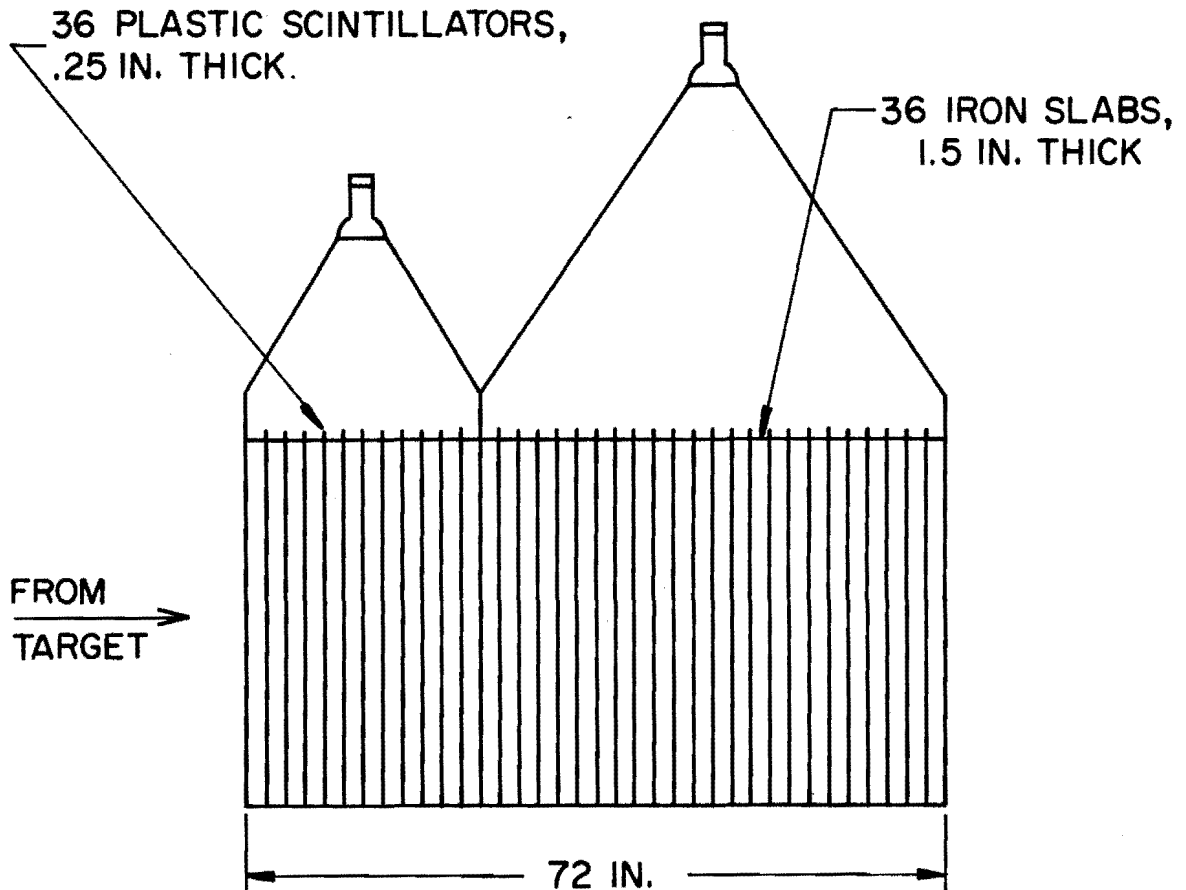


FIGURE 1

FIG. 2. TRIAL VERSION OF 90° CALORIMETER



a) FRONT VIEW OF 90° CALORIMETER



b) SCHEMATIC SIDE ELEVATION

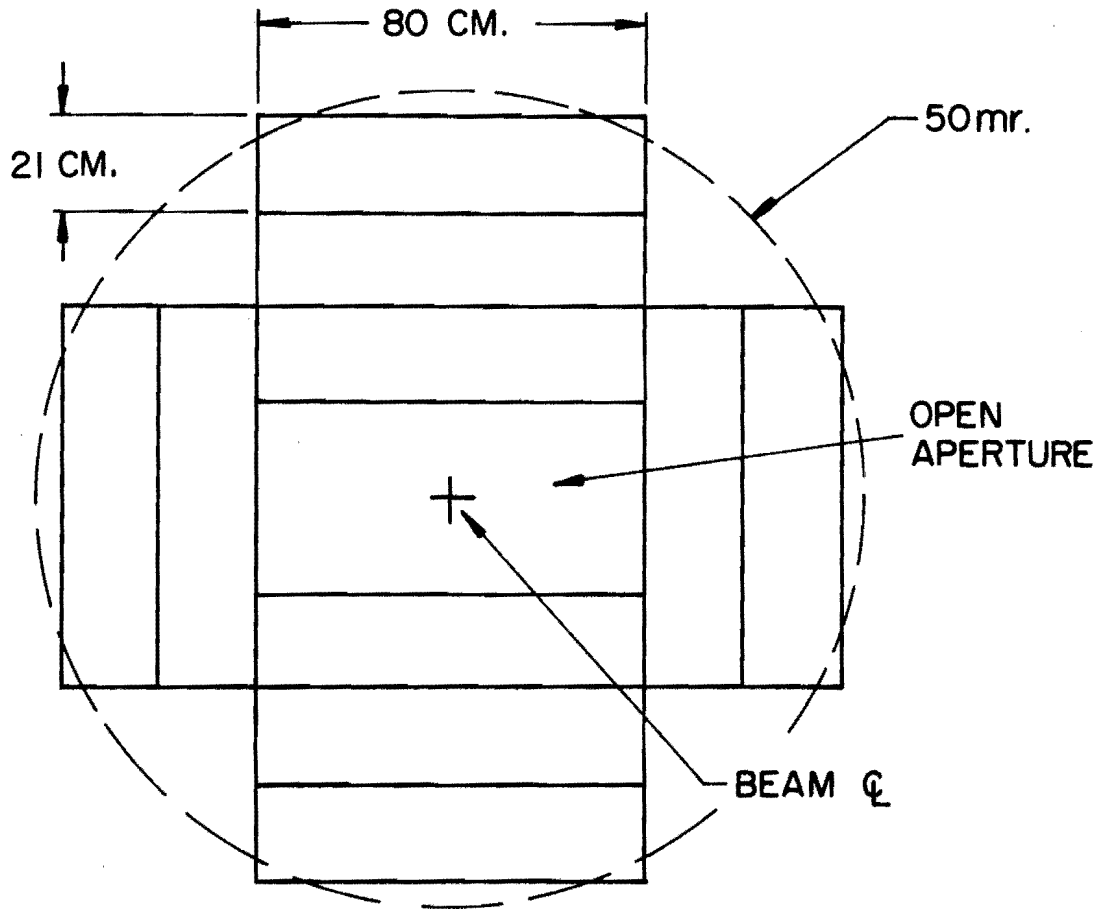


FIGURE 3
FRONT VIEW OF TRIAL FORWARD CALORIMETER

SOLID ANGLE ACCEPTED FOR $60^\circ < \theta_{c.m.} < 120^\circ$

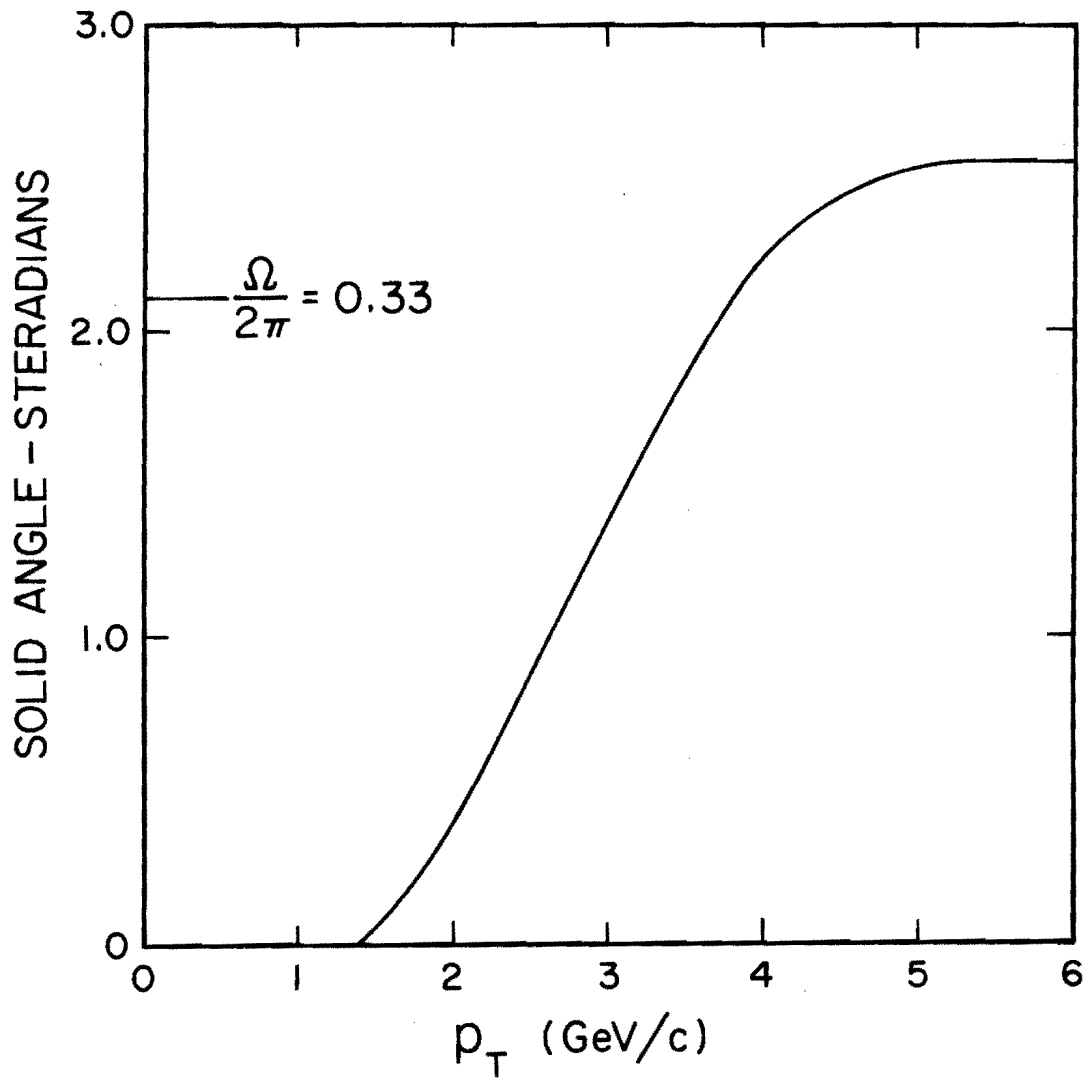
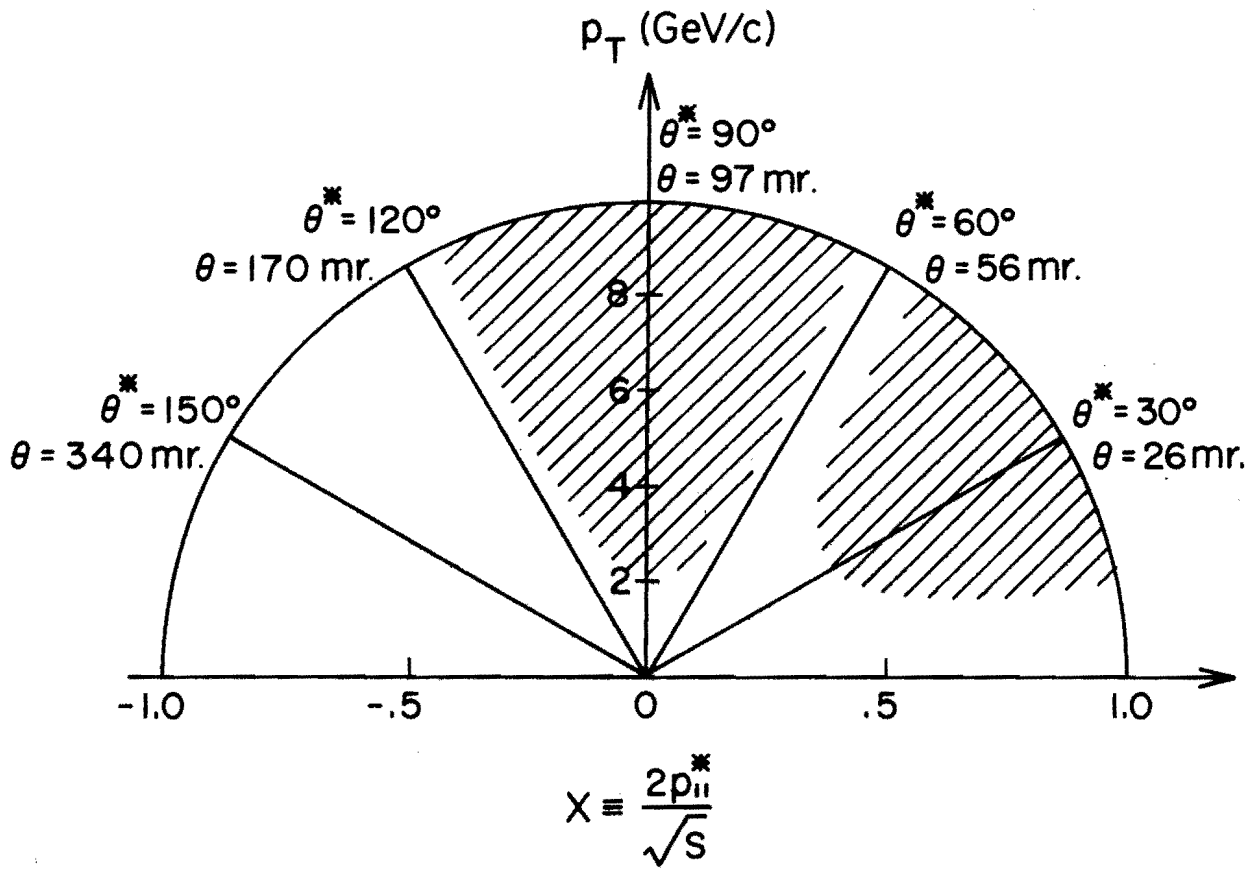


FIGURE 4



Kinematics in c.m. and lab. The shaded areas are regions of good trigger acceptance.

FIGURE 5

ADDENDUM TO E260:

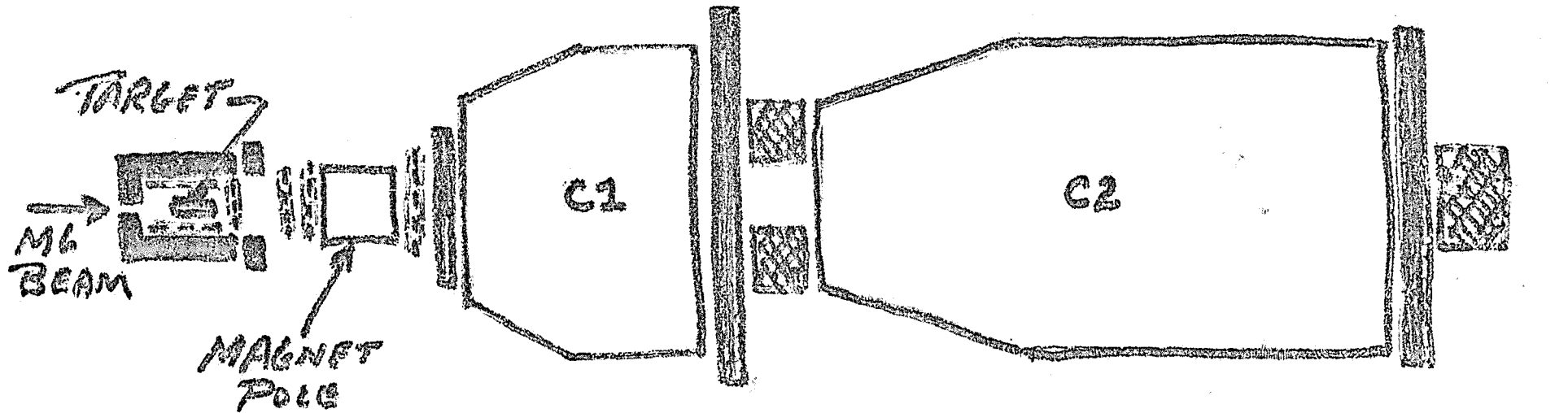
STUDY OF HIGH MASS PARTICLES

(A Pictorial Summary)

December 9, 1974

PROPOSAL # 260.
MASTER
DO FILE
ELG
JRS

MULTIPARTICLE SPECTROMETER FACILITY



2M

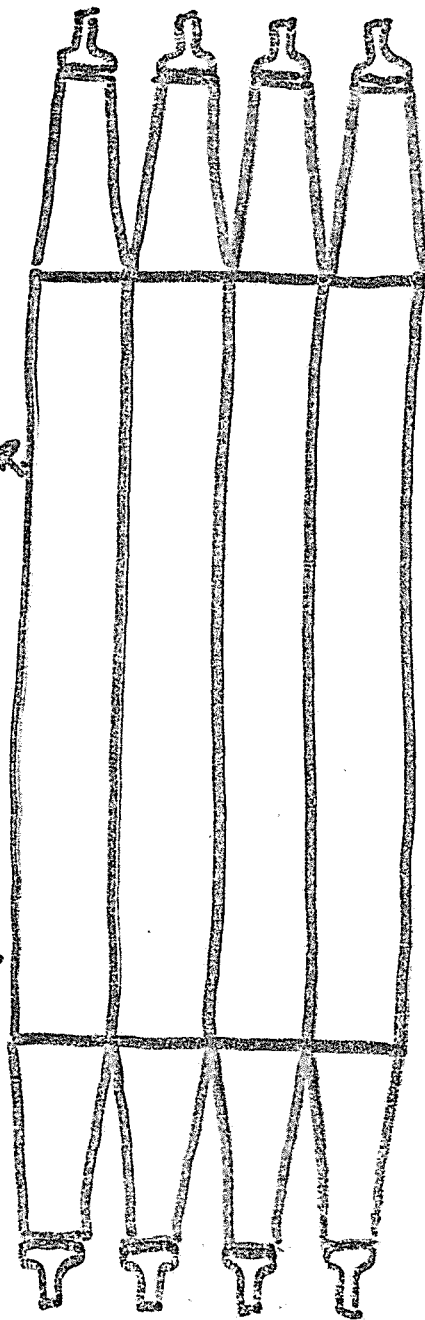
KEY

- MWPC
- LEAD-SCINTILLATOR
- WIRE SPARK CHAMBERS
- CALORIMETERS

"90°" CALORIMETERS

PM TUBE
OUTPUTS
WEIGHTED,
FOR P_{\perp} TRIGGER

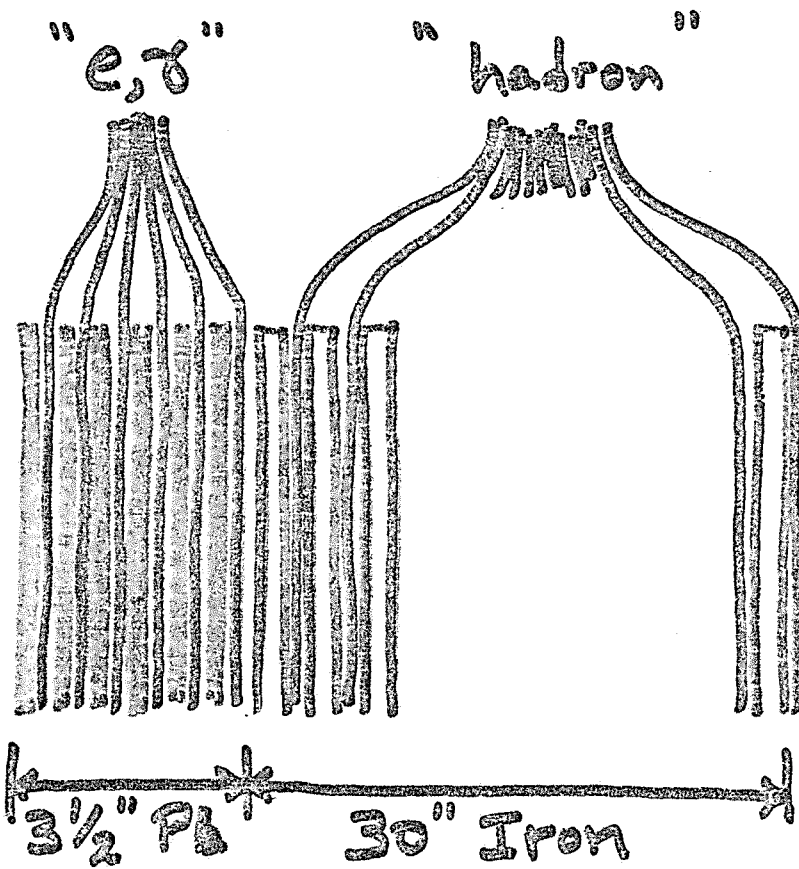
RATIO OF TOP
& BOTTOM PM
TUBE OUTPUTS
GIVES VERTICAL
POSITION.



+
BEAM

1 m.

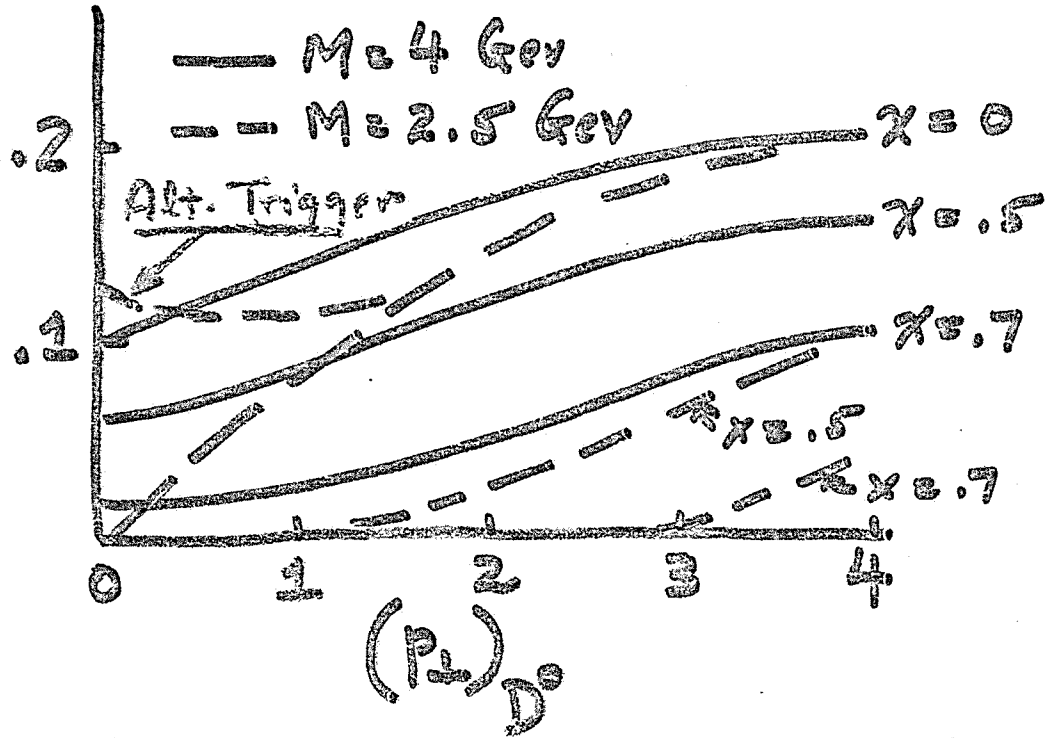
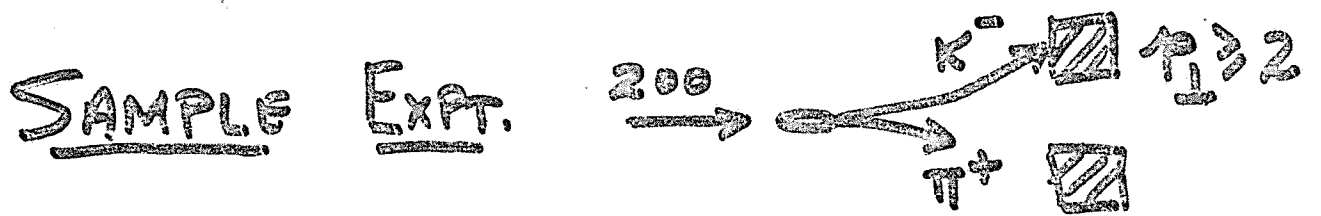
CALORIMETER SCHEMATIC
SIDE VIEW



→
BEAM
DIRECTION

MAIN FEATURES

1. M6 Beam (π , P, (K?)).
2. FLEXIBLE TRIGGERING
3. LARGE ACCEPTANCE - EVEN FOR 3, 4-BODY DECAYS
4. LARGE RANGE OF M_s AND OF (P_L, X) AT PRODUCTION.
5. GOOD PARTICLE IDENTIFICATION
6. FLEXIBLE GEOMETRY
7. EARLY OPERATION (?)

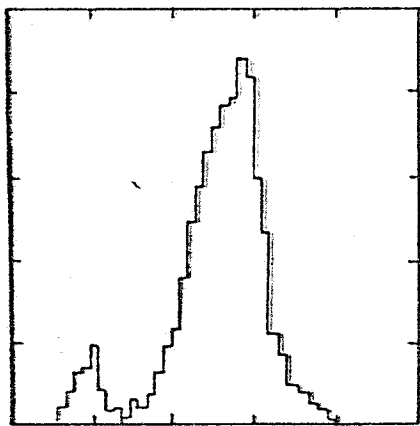


$$\text{Rate}/nb \sim 1/\text{hour}$$

$$(4 \text{ g. H}, 5 \times 10^6/\text{pulse})$$

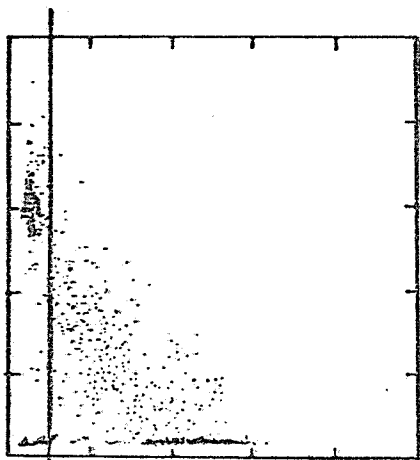
$$\Delta M \approx 10 - 20 \text{ MeV.}$$

17 GeV



$P_{He} + P_{Hh}$

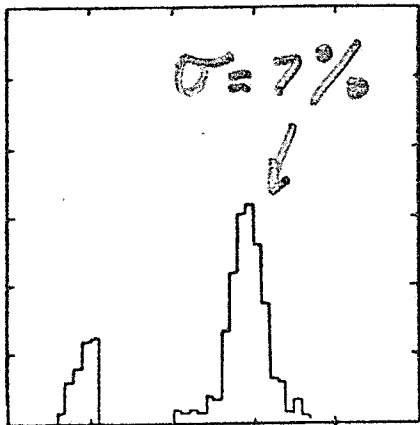
$$\left(\frac{\Delta E}{E}\right)_{e,\delta} = \frac{.28}{\sqrt{E_{GeV}}}$$



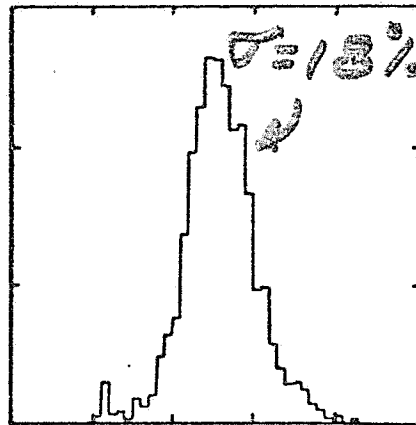
P_{He}

P_{Hh}

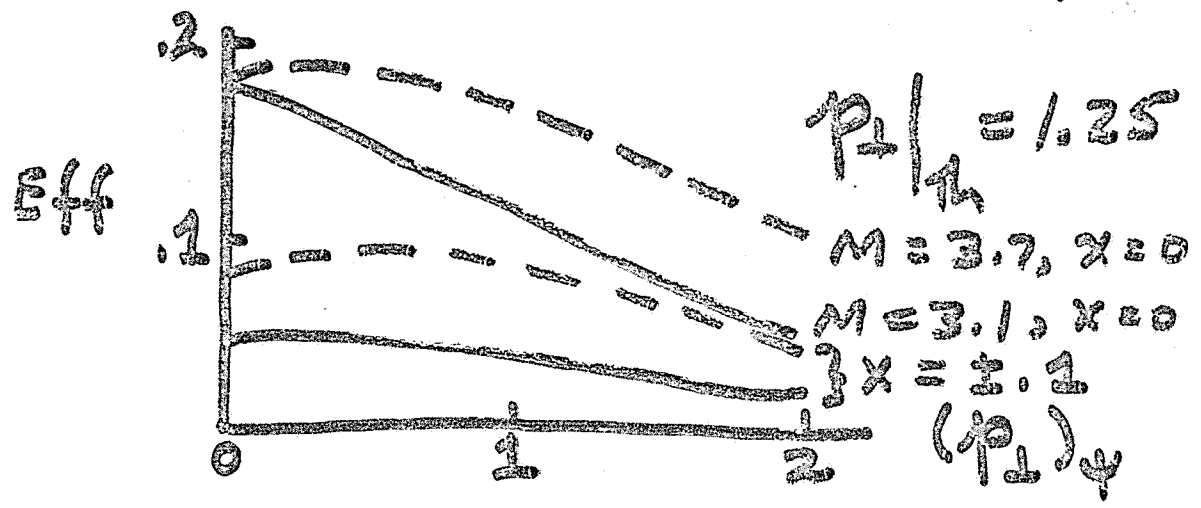
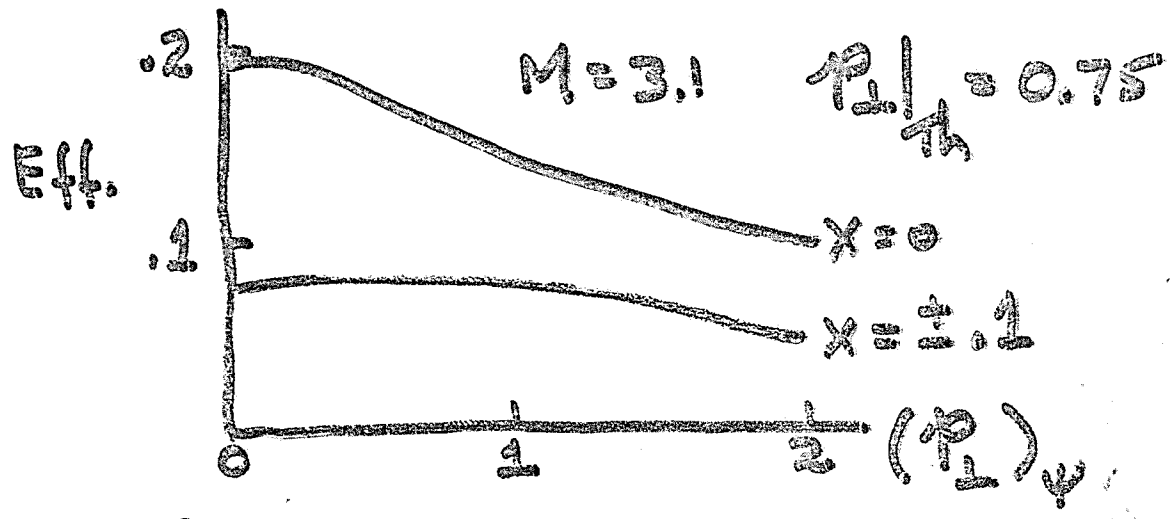
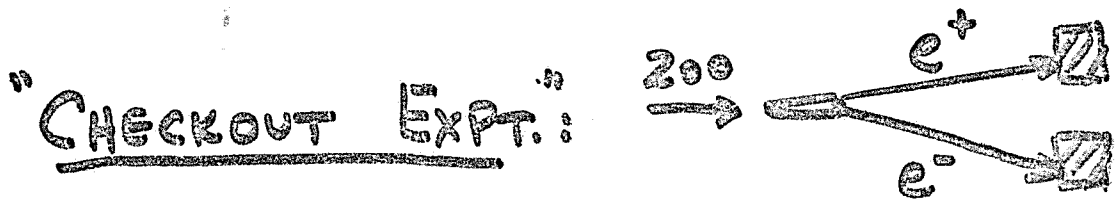
$$\left(\frac{\Delta E}{E}\right)_{hadron} = \frac{.72}{\sqrt{E_{GeV}}}$$



$P_{He} + P_{Hh}$



$P_{He} + P_{Hh}$



Rate/nanob. \approx ? 1 / Hour
 (59. Be, 10^7 /pulse)

$\Delta M \approx \pm 150$ Mev.